Composition controlling the number of absorption peaks in three-layered metal-dielectric-metal nanoshell

GUOJUN WENG, JIANJUN LI, JUNWU ZHAO*
The Key Laboratory of Biomedical Information Engineering of Ministry of Education, School of Life Science and Technology, Xi'an Jiaotong University, No. 28 Xianning West Road, Xi'an 710049, China

The number change of absorption peaks of three-layered nanoshells have been investigated in theory with variation of the composition. With an increase of the gold content in the inner core and outer shell, the number of absorption peaks changed from three to two and from one to two, respectively. And the corresponding physical mechanism had been discussed. The number tunability of peaks coming from the composition was affected by the geometrical parameters and the dielectric constant. This composition dependent number change of peaks would provide insights to synthesis and designing of three-layered nanoshells sensors for multi-molecular sensing.

(Received April 2, 2015; accepted April 5, 2016)

Keywords: Au/Ag alloy, Quasistatic approximation, Three-layered nanoshells, Number tunability of absorption peaks

1. Introduction

Gold and silver nanostructures have numerous promising applications in the field of biology and medicine due to their fascinating electronic and optical properties that are known as the localized surface plasmon resonance (LSPR) [1-4]. The frequency of LSPR can be controlled over a wide range by variation of the size, shape, dielectric surrounding, and composition of the nanoparticles [5, 6]. Furthermore, the assembly and aggregation pattern of gold or silver nanoparticles suspending in solution or absorbing on substrates is also an important factor in the tuning of LSPR [7, 8]. The easy and extensive controlling of LSPR makes gold and silver nanostructures perfect nanoprobes in biosensing and diagnostics.

In early disease diagnosis, testing only one biomarker is not enough to confirm a disease. For example, primary hepatocellular carcinoma, a positive result of α-fetoprotein (AFP) in human blood is not sufficient to diagnose, always needing extra tests for checking other biomarkers [9, 10]. Detecting one biomarker at a time for diagnosis one disease leads to high costs and time-consuming. Thus, there has been a continuously growing interest in developing new methods and devices that can provide simultaneous detection of different disease biomarkers at one round testing. Gold nanorods with transverse and longitudinal plasmon bands had been used to detecting several different biomarkers at a time, showing a potential for multiplexed bioassay [11, 12]. In their research, detecting one biomarker used one type of gold nanorods. Thus, gold nanorods with different aspect ratios should be prepared for detecting different biomarkers. In my opinion, the important prerequisite for multi-targets assay using noble nanoparticles is that the number of LSPR peaks should match the number of biomarkers. In other words, each LSPR peaks represents one biomarkers. For multi-assay with targets more than three, the used nanoprobes must be able to offer appropriate number of peaks for signals acquiring. Therefore, fabricating gold or silver nanostructures with three or more LSPR bands is essential for early diagnosis of diseases with multiplex biomarkers.

Recently, three-layered gold nanostructures have been synthesized [13, 14] and their LSPR are being extensively investigated [14-24]. According to the theory of plasmon hybridization [25], three-layered gold nanoshells may have four LSPR peaks in theory due to the plasmon coupling between the inner core and outer shell. The plasmon coupling leads to two kinds of mode: the anti-bonding and bonding mode [19]. The anti-bonding mode of the outer gold nanoshell divided into two plasmon modes. The first is anti-symmetric coupling between the anti-bonding outer gold shell and the inner gold core, denoted as $|\omega_+^+\rangle$ mode. The second is symmetric coupling between the anti-bonding outer gold shell and the inner gold core, denoted as $|\omega_+^-\rangle$ mode. On the other hand, the bonding mode of the outer gold nanoshell also divided into two plasmon modes: the higher energy symmetric anti-bonding mode $|\omega_-^+\rangle$ and the lower energy antisymmetric bonding mode $|\omega_-^-\rangle$. However, the energy of $|\omega_+^+\rangle$ mode is too weak, leading to no absorption band being observed. Furthermore, the absorption band corresponding to $|\omega_+^-\rangle$ mode only displays on extreme condition [19].

With different geometrical parameters and local dielectric constants, the number of LSPR peaks in three-layered nanoshells varied from one to three [19, 22]. Qian *et al.* [18] found that reducing the distance between the gold inner core and the gold outer shell in three-layered nanoshells leaded the conversion from $|\omega_{-}^{+}\rangle$ to $|\omega_{+}^{-}\rangle$ mode. This indicated that the LSPR peaks number of three-layered nanoshell could also be controlled by the thickness of middle layer. In addition, Zhu *et al.* [20] found that the absorption band corresponding to $|\omega_{+}^{-}\rangle$ mode could be enhanced by replacing the composition of outer gold shell with silver. Inspired by the work of Zhu *et al.* [20], we investigates the number change of absorption peaks in metal-dielectric-metal nanoshells with variation of the composition of the inner core and outer shell. The calculations show that the number of LSPR peaks of three-layered nanoshells is tunable by altering the composition both in the inner core and outer shell. Also, we discuss in detail the influence of geometrical parameters and local dielectric constants on the number tunability of LSPR peaks coming from the composition.

2. Methods

We investigate the number changing of LSPR peaks controlled by the composition of metal layer in three-layered nanoshells. Geometry of the structure of three-layered metal nanoshell is shown in Fig. 1. The three-layered nanostructure is composed of three parts: the inner and outer Au/Ag alloy layer, and the middle dielectric layer. The radius of inner Au/Ag alloy core is R_1 and its dielectric constant is ε_1. The thickness and the dielectric constant of the middle dielectric layer is $R_2 - R_1$ and ε_2 respectively. The outer Au/Ag alloy shell has a thickness $R_3 - R_2$ and a dielectric constant ε_3. The whole metal-dielectric-metal nanoshell is embedded in the medium with a dielectric constant ε_4. In this paper, the overall radius R_3 of the three-layered nanoshell is fixed at 25 nm, which is much smaller than the wavelength of incident light. Thus, the absorption spectra of the three-layered nanoshell can be calculated by using the quasistatic approximation of classical electrodynamics. According to the Drude model [22, 26, 27], the wavelength-dependent complex dielectric function (ε_1 and ε_3) of the inner and outer Au/Ag alloy layer can be written as follow:

$$\varepsilon_1(\omega) = \varepsilon_3(\omega) = \varepsilon_r + i\varepsilon_i = \varepsilon_b(\omega) - \frac{\omega_p^2/\omega^2}{1+(1/\omega^2\tau^2)} + i\frac{\omega_p^2/\omega^2}{\omega\tau+(1/\omega\tau)} \quad (1)$$

where

$$\varepsilon_b(\omega) = p\varepsilon_{bAu} + (1-p)\varepsilon_{bAg} \quad (2)$$

$$\omega_p = p\omega_{pAu} + (1-p)\omega_{pAg} \quad (3)$$

$$\tau = p\tau_{Au} + (1-p)\tau_{Ag} \quad (4)$$

In the above equations, p is the molar composition of gold with a range of zero to one; ω_{bAu} and ω_{bAg} are the bulk dielectric data of pure Au and Ag; τ_{Au} and τ_{Ag} are also the relaxation time of pure Au and Ag [28]. In this work, the size of the three layered gold nanoshells is similar to the bulk electron mean free path [29], a contribution to the dielectric function that is due to electron surface scattering becomes important. Thus, the size limit relaxation time (τ) depends on the limited mean free path of the electrons [17, 26]. However, for simplifying the calculation, we chose the limit relaxation time τ_{Au} = 9.8 fs and τ_{Ag} = 3.1 fs, respectively [22]. The parameters used in the calculations are obtained from the ref. [30, 31].

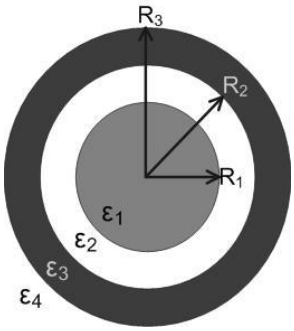

Fig. 1. Geometry of the structure of three-layered gold nanoshell

According to the quasistatic approximation theory, the absorption cross section of the core-shell structure gold nanoshell is given as follows:

$$\sigma_{abs} = \frac{k}{\varepsilon_0}\mathrm{Im}(\alpha) \quad (5)$$

where $k = 2\pi\sqrt{\varepsilon_4}/\lambda$, ε_0 is the permittivity of free space, and α is the polarizability of three-layered gold nanoshell, which can be obtained in our previous work [21, 22]. In the present work, two cases were calculated: (1) the inner core was alloy of Ag and Au while the outer shell was pure Au (Ag/Au@Au); (2) the outer shell was alloy of Ag and Au while the inner core was pure Au (Au@Ag/Au).

3. Results and discussion

3.1 Changing the composition of inner core

The calculated absorption of three-layered nanoshell with different inner core composition is shown in Fig. 2. Fig. 2(a) shows the absorption spectra of three-layered nanoshell with the geometrical factor [R_1=15, R_2=22, R_3=25 nm] and the dielectric constant [ε_2=2, ε_4=2]. As the Au content of inner core (p) increased, the $|\omega_{+}^{-}\rangle$ and

$|\omega_{-}^{+}\rangle$ mode blended together and turned in to one peak at last. The Ag inner core (p=0) configuration had three LSPR peaks while the Au inner core (p=1) configuration had two LSPR peaks under the same geometrical parameters and surrounding medium. Additionally, the intensity of the $|\omega_{-}^{+}\rangle$ mode was consistent with the increase of inner core Au content, but the change of the $|\omega_{-}^{-}\rangle$ mode intensity was limited. Fig. 2(b) is the calculated absorption spectra of three-layered nanoshell with [R_1=10, R_2=17, R_3=25 nm] and [ε_2=2, ε_4=2]. As the molar composition p enhanced, the mode $|\omega_{-}^{+}\rangle$ appeared and became strong. The number of LSPR peaks changed form one to two when the composition of inner core varied from Ag to Au. The calculated results confirmed the potential effect of nanoshell composition on the plasmon hybridization and the controlling of LSPR peaks number.

The inner core size can also control the number of LSPR peaks for three-layered nanoshell of different Au content. When the inner core size ranged from 5 to 20 nm, the number of LSPR peaks varied from one to three, as shown in Fig. 3(a). However, the number of LSPR peaks varied significantly just as Au content was below 0.3. Furthermore, the turning ability of inner core composition on LSPR peaks just worked under a big inner core size. The effect of the outer shell thickness on the inner core composition turning ability in the three-layered nanoshells had been investigated, as shown in Fig. 3(b). When R_2 ranged from 16 to 24 nm, the number of LSPR peaks changed from one to three. In most case, the number of LSPR peaks was two, one or three, and just appearing at low odd. As the value of p was high, R_2 had little influence on the number of LSPR peaks.

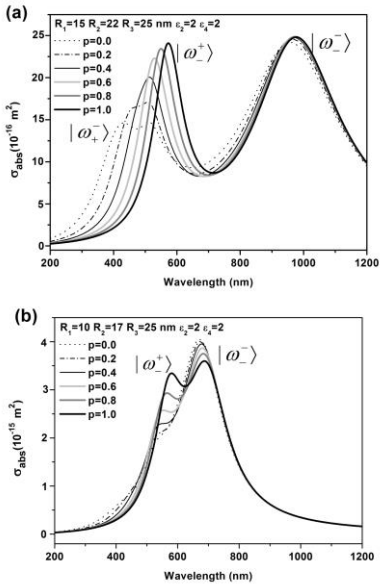

Fig. 2. Absorption spectra of three-layered nanoshell with different molar composition of gold in the inner core. (a) R_1=15, R_2=22, R_3=25 nm, ε_2=2, ε_4=2; (b) R_1=10, R_2=17, R_3=25 nm, ε_2=2, ε_4=2.

The dielectric constant of the middle layer also has effect on the number of LSPR peaks when changing the inner core composition. As shown in Fig. 3(c), the number of LSPR peaks increased from one to three as the ε_2 increasing. When ε_2 was below 5, the Au content of inner core (p) had no obvious influence on the number of the LSPR peaks. However, as ε_2 was above 5, the number of LSPR peaks had a drastic change, varying from two to one and then to three. These results indicated that the number of LSPR peaks in three-layered nanoshells was easy to control by the inner core composition when the middle layer had a high value of the dielectric constant.

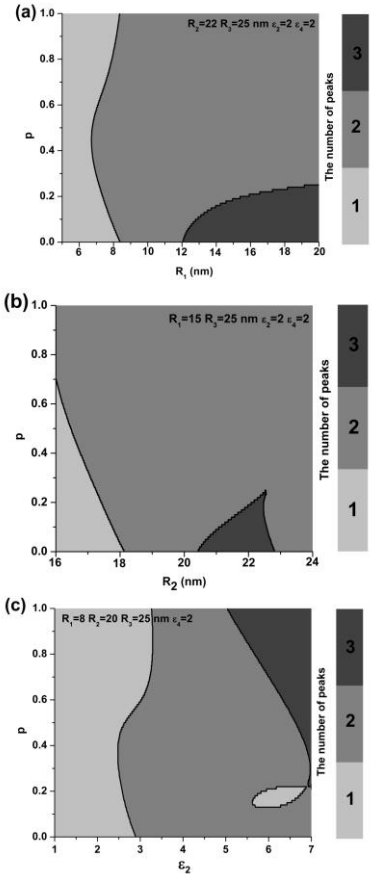

Fig. 3. The number of absorption peak as a function of gold molar composition and (a) R_1, (b) R_2, (c) ε_2.

3.2 Changing the composition of outer shell

In this part, we investigated the influence of the outer shell composition on the number changing of LSPR peaks. The wavelength variations of absorption cross section for three-layered nanoshell structures of different outer compositions with a fixed thickness of 3 nm were shown in Fig. 4(a). When the Au content of outer core (p) increased, the $|\omega_{+}^{-}\rangle$ and $|\omega_{-}^{+}\rangle$ mode shifted to longer wavelength and intensity of both peaks gradually decreased, while the $|\omega_{-}^{-}\rangle$ mode shifted to shorter wavelength and its intensity increased. The influence of the outer shell composition on the $|\omega_{+}^{-}\rangle$ and $|\omega_{-}^{-}\rangle$ mode was distinctly greater than the $|\omega_{-}^{+}\rangle$ mode. The number of

LSPR peaks in three-layered nanoshells changed from three to two with increasing the Au content in outer shell under the same geometrical parameters and surrounding medium. In Fig. 4(b), the geometrical factor and the dielectric constant used for calculation were [R_1=10, R_2=17, R_3=25 nm] and [ε_2=2, ε_4=2], respectively. As the molar composition p enhanced, the $|\omega_-^-\rangle$ mode gradually displayed and its intensity became strong. The number of LSPR peaks was tuned from one to two by increasing the gold composition. Thus, the results shown in Fig. 4 suggested that the number of LSPR peaks also depended on the composition of outer shell.

In Fig. 5(a) we show the effect of increasing in the inner core radius on the number of LSPR peaks for a given outer shell thickness with increasing the Au content. When the inner core had larger radius, the distribution of the LSPR peaks number was divided into three regions, which was similar to that of the first case. When the radius of inner core below 10 nm, increasing the Au content in outer shell had no influence on the number of LSPR peaks. However, as the radius of inner core increased from 10 to 20 nm, the number of LSPR peaks decreased from three to two with the enhancement of Au content. Therefore, the regulation of the LSPR peaks number from the composition of outer shell was effective for large radius of inner core.

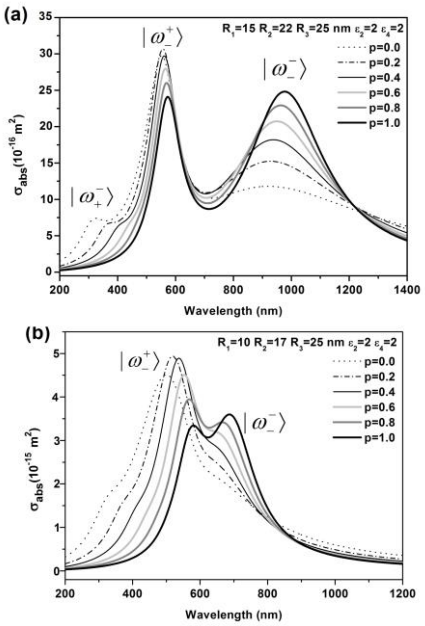

Fig. 4. Absorption spectra of three-layered nanoshell with different molar composition of gold in the outer shell. (a) R_1=15, R_2=22, R_3=25 nm, ε_2=2, ε_4=2; (b) R_1=10, R_2=17, R_3=25 nm, ε_2=2, ε_4=2.

We further investigated the variation of the number of LSPR peaks with the outer layer thickness ranging from 9 to 1 nm. Here, the inner core radius R1 and the overall radius R3 were fixed at 15 and 25 nm, respectively. As shown in Fig. 5(b), with decreasing the outer layer thickness the number of LSPR peaks increased from one to three. When the thickness of the outer shell was above 5 nm, the number of LSPR peaks changed from one to two with increasing the Au content. However, the number of LSPR peaks changed from three to two with very thin outer shell. As the Au content of the outer shell was low, the number of three-layered nanoshells was easy to control by changing the thickness of the outer shell.

Finally, we investigated the influence of the dielectric constant for the middle dielectric layer on the LSPR peaks number controlling by the outer shell composition. Fig. 5(c) showed the distribution of the LSPR peaks number versus the dielectric constant (ε_2) and the Au content in the outer shell. When the Au content in the outer shell was high, the number of LSPR peaks increased from one to three with increasing ε_2. When ε_2 was below 2.5, the number of LSPR peaks was lower than that of ε2 being above 2.5 with increasing the Au content. As seen from Fig. 5(c), the influence of the dielectric constant on the tuning the number of LSPR peaks by outer shell composition was power than that of the inner core size and the outer shell thickness. The results indicated that the type of the middle layer played an important in the controlling the number of LSPR peaks by the outer shell composition.

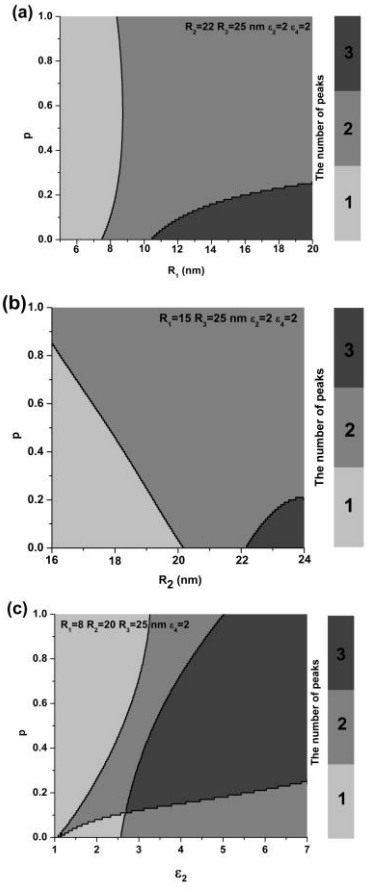

Fig. 5. The number of absorption peak as a function of gold molar composition and (a) R_1, (b) R_2, (c) ε_2.

3.3 The mechanism of composition dependent number change of LSPR peaks

Tuning the LSPR band number of silver ellipsoidal nanoshell [32] and gold coated aluminum nanorods [33] had been reported previously. The mechanism of LSPR peak number changing was due to the anisotropic plasmon splitting and the plasmon coupling. Furthermore, the number changing and shifting of absorption peaks was observed in the spherical nanoparticles with quantum spatial dispersion [34, 35]. With considering the quantum effects, the number of subsidiary peaks changed from two to one (R=1 nm) and four to three (R=2 nm). However, the number of subsidiary peaks increased in both nonlocal models (the standard theory and the quantum theory). The observed extinction properties of nanospheres were dependent on the quantum effects, including Fermi pressure and quantum diffraction. The positions and number of the subsidiary peaks exhibited strong dependence on the quantum spatial dispersion.

In this paper, we talked about the number change of LSPR bands in three-layered nanoshells with variation of composition in inner core and outer shell. For three-layered nanoshell with [R_1=15, R_2=22, R_3=25 nm] and [ε_2=2, ε_4=2], the $|\omega_+^-\rangle$ mode blended with the $|\omega_-^+\rangle$ mode or just disappeared as the composition changed from Ag to Au in two cases, as shown in Fig. 2(a) and Fig. 4(a). Thus, the number of LSPR peaks changing from three to two was related to the variation of the $|\omega_+^-\rangle$ mode. In the three-layered gold nanoshells, the $|\omega_+^-\rangle$ mode is very weak due to the opposite aligning between the cavity plasmon of the inner surface and the sphere plasmon of the outer surface in the gold shell. However, the inner sphere plasmon enhances the dipole moment of the $|\omega_+^-\rangle$ mode [19, 20]. It is known that the LSPR band of silver nanoparticles is stronger and sharper than that of gold nanoparticles [36]. When the Au content increased and Ag content decreased in inner core, the enhancement form the inner sphere plasmon to the dipole moment of the $|\omega_+^-\rangle$ mode becomes weak and blended with the $|\omega_-^+\rangle$ mode. Thus, the $|\omega_+^-\rangle$ mode shifts to red and gradually disappeared at last, as shown in Fig. 2(a). In the other hand, the plasmon of the outer shell shows a greater influence on the total plasmon of the multi-shells [20]. Furthermore, compared with the outer gold nanoshell, the charge density and the local field of the outer silver shell are much greater [20]. When the Au content increased and Ag content decreased in outer shell, the influence of the plasmon of outer shell on the dipole moment of $|\omega_+^-\rangle$ mode becomes weak, and the charge density and the local field of the outer shell also decreased. Therefore, the $|\omega_+^-\rangle$ mode also shifts to red and gradually disappeared, as shown in Fig. 4(a). So, the number of LSPR peaks changed from three to two when the composition in inner core and outer shell was changed.

For three-layered nanoshell with [R_1=10, R_2=17, R_3=25 nm] and [ε_2=2, ε_4=2], there was one strong band when the inner core or outer shell was Ag, as shown in Fig. 2(b) and Fig. 4(b). However, as the Au content increased in both cases, the $|\omega_-^+\rangle$ mode displayed in Fig. 2(b), while the $|\omega_-^-\rangle$ mode appeared in Fig. 4(b). Thus, the number of LSPR peaks changing from one to two was attributed to the appearance of the $|\omega_-^+\rangle$ and $|\omega_-^-\rangle$ mode in two cases. In Au-Ag alloy nanotubes, the increase of gold molar composition leaded to the red shift of both two peaks, and the peak with short wavelength was more sensitive to the change in Au composition [28]. In other words, the shift speed of the two LSPR peaks was different when increasing gold molar composition. Furthermore, the different shift blue speed of the LSPR peaks would make the plasmon blending, which decreased the number of LSPR peaks [32]. In this report, as the Au content increased in inner core and outer shell, the $|\omega_-^+\rangle$ and $|\omega_-^-\rangle$ mode both shifted to red, and the shift speed of $|\omega_-^+\rangle$ mode was faster. In Fig. 2(b), the $|\omega_-^+\rangle$ mode shifted to red faster and was squeezed to a new peak; while in Fig. 4(b), the $|\omega_-^-\rangle$ mode shifted to red slower and was squeezed to a new peak too. Therefore, the number of LSPR increased from one to two as the the increase of gold molar composition in inner core and outer shell.

4. Conclusions

In conclusion, we have investigated the number change of LSPR peaks controlled by the composition of the inner core and outer shell in three-layered nanoshells. The calculations suggested that the number of LSPR peaks was tunable by the composition of the inner core and outer shell. Also, the effect of the inner core size, the outer shell thickness, and the dielectric constant of middle layer on the number tunability with nanoshells composition was studied in details. Compared with the size of the inner core and outer shell, the dielectric constant of middle layer had more obvious impact on the number tunability of LSPR peaks. This tunable number changing of LSPR peaks by nanoshells composition offered insight to the fabricating nanoshells sensors for multi-targets detection.

Acknowledgements

This work was supported by the National Natural Science Foundation of China (Grant Nos. 21403161 and 61178075) and the China Post-doctoral Science Foundation (Grant No. 2014M552433). G.W. acknowledges the support from Xi'an Jiaotong University Faculty Research Grant.

References

[1] S. S. Lucky, K. C. Soo, Y. Zhang, Chem. Rev. **115**,

1990 (2015).
[2] D. A. Giljohann, D. S. Seferos, W. L. Daniel, M. D. Massich, P. C. Patel, C. A. Mirkin, Angew. Chem. Int. Ed. **49**, 3280 (2010).
[3] B. Pelaz, S. Jaber, D. J. de Aberasturi, V. Wulf, T. Aida, J. M. de la Fuente, J. Feldmann, H. E. Gaub, L. Josephson, C. R. Kagan, N. A. Kotov, L. M. Liz-Marzán, H. Mattoussi, P. Mulvaney, C. B. Murray, A. L. Rogach, P. S. Weiss, I. Willner, W. J. Parak, Acs Nano **6**, 8468 (2012).
[4] P. D. Howes, S. Rana, M. M. Stevens, Chem. Soc. Rev. **43**, 3835 (2014).
[5] K. L. Kelly, E. Coronado, L. L. Zhao, G. C. Schatz, J. Phys. Chem. B **107**, 668 (2003).
[6] P. K. Jain, K. S. Lee, I. H. El-Sayed, M. A. El-Sayed, J. Phys. Chem. B **110**, 7238 (2006).
[7] P. K. Jain, M. A. El-Sayed, Chem. Phys. Lett. **487**, 153 (2010).
[8] L. B. Wang, Y. Y. Zhu, L. G. Xu, W. Chen, H. Kuang, L. Q. Liu, A. Agarwal, C. L. Xu, N. A. Kotov, Angew. Chem. Int. Ed. **49**, 5472 (2010).
[9] F. A. Durazo, L. M. Blatt, W. G. Corey, J. H. Lin, S. Han, S. Saab, R. W. Busuttil, M. J. Tong, J. Gastroenterol. Hepatol. **23**, 1541 (2008).
[10] D. Li, T. Mallory, S. Satomura, Clin. Chim. Acta **313**, 15 (2001).
[11] H. Huang, F. Liu, S. Huang, S. Yuan, B. Liao, S. Yi, Y. Zeng, P. K. Chu, Anal. Chim. Acta **755**, 108 (2012).
[12] C. X. Yu, J. Irudayaraj, Anal. Chem. **79**, 572 (2007).
[13] X. H. Xia, Y. Liu, V. Backman, G. A. Ameer, Nanotechnology **17**, 5435 (2006).
[14] R. Bardhan, S. Mukherjee, N. A. Mirin, S. D. Levit, P. Nordlander, N. J. Halas, J. Phys. Chem. C **114**, 7378 (2009).
[15] Y. Hu, R. C. Fleming, R. A. Drezek, Opt. Express **16**, 19579 (2008).
[16] D. J. Wu, X. D. Xu, X. J. Liu, J. Chem. Phys. **129**, 074711 (2008).
[17] D. J. Wu, X. J. Liu, Appl. Phys. B-Lasers Opt. **97**, 193 (2009).
[18] J. Qian, Y. Li, J. Chen, J. Xu, Q. Sun, J. Phys. Chem. C **118**, 8581 (2014).
[19] J. Zhu, J. J. Li, J.W. Zhao, Plasmonics **6**, 527 (2011).
[20] J. Zhu, J. J. Li, L. Yuan, J. W. Zhao, J. Phys. Chem. C **116**, 11734 (2012).
[21] J. Zhu, Y. J. Ren, S. M. Zhao, J. W. Zhao, Mater. Chem. Phys. **133**, 1060 (2012).
[22] G. Weng, J. Li, J. Zhao, Physica E **44**, 2072 (2012).
[23] A. Moradi, J. Opt. Soc. Am. B **29**, 625 (2012).
[24] Y. Zhang, G. T. Fei, L. D. Zhang, J. Appl. Phys. **109**, 054315 (2011).
[25] E. Prodan, C. Radloff, N. J. Halas, P. Nordlander, Science **302**, 419 (2003).
[26] R. D. Averitt, S. L. Westcott, N. J. Halas, J. Opt. Soc. Am. B: Opt. Phys. **16**, 1824 (1999).
[27] J. Zhu, Appl. Phys. Lett. **92**, 241919 (2008).
[28] J. Zhu, J. Phys. Chem. C **113**, 3164 (2009).
[29] N. W. Ashcroft, N. D. Mermin, Solid State Physics, Holt, Rinehart and Winston, New York, 1976.
[30] P. B. Johnson, R. W. Christy, Phys. Rev. B **6**, 4370 (1972).
[31] D. Canchal-Arias, P. Dawson, Surf. Sci. **577**, 95 (2005).
[32] J. Zhu, X. C. Deng, J. J. Li, J. W. Zhao, J. Nanopart. Res. **13**, 953 (2011).
[33] J. Zhu, J. J. Li, J. W. Zhao, Phys. Plasmas **21**, 112108 (2014).
[34] A. Moradi, Surf. Sci. **637–638**, 53 (2015).
[35] A. Moradi, Phys. Plasmas **22**, 022119 (2015).
[36] D. J. Wu, X. J. Liu, Appl. Phys. Lett. **96**, 151912 (2010).

*Corresponding author: nanoptzhao@163.com